The role of tin and iron in the production of Spanish copper red glass from the 19th to the 20th century

Mingyue Yuan, Jordi Bonet, Hiram Castillo-Michel, Marine Cotte, Nadine Schibille, Bernard Gratuze, Trinitat Pradell

BOLETIN DE LA SOCIEDAD ESPAÑOLA DE
Cerámica y Vidrio
www.elsevier.es/bsecv

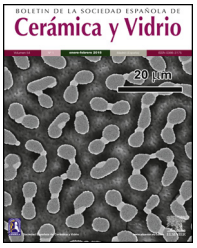

Original

The role of tin and iron in the production of Spanish copper red glass from the 19th to the 20th century

Mingyue Yuan[a], *Jordi Bonet*[b], *Hiram Castillo-Michel*[c], *Marine Cotte*[c,d], *Nadine Schibille*[e], *Bernard Gratuze*[e], *Trinitat Pradell*[a,*]

[a] *Physics Department and Barcelona & Research Centre in Multiscale Science and Engineering, Universitat Politècnica de Catalunya, BarcelonaTech, Campus Diagonal Besòs, c) Av. Eduard Maristany 16, 08930 Barcelona, Spain*
[b] *J.M. Bonet Vitralls S.L., c) Corominas 17, 08902 L'Hospitalet de Llobregat, Barcelona, Spain*
[c] *ESRF, The European Synchrotron, CS 40220, 38043 Grenoble Cedex 9, France*
[d] *Laboratoire d'Archéologie Moléculaire et Structurale (LAMS), CNRS, UMR 8220, Sorbonne Université, UPMC University Paris 06, 4 Place Jussieu, 75005 Paris, France*
[e] *Institut de Recherche sur les Archéomatériaux (IRAMAT), UMR 7065, CNRS/Université d'Orléans, Centre Ernest Babelon, Orléans, France*

ARTICLE INFO

Article history:
Received 24 April 2023
Accepted 23 July 2023
Available online 12 August 2023

Keywords:
Metallic copper nanoparticles
Cu, Fe K-edge and Sn L_3-edge
Micro-XAS
Micro-XRD
19th and 20th window glass
Spain

ABSTRACT

Little is known about the materials used in the manufacture of red window glass in the 19th and the first decade of the 20th century. Here, we have studied fragments from eight Spanish glasses from the 19th and 20th centuries. The red glasses consist of a single layer of red glass on a colourless glass substrate. The chemical composition, oxidation state, nature of colourants and crystalline precipitates were determined by a selection of microanalytical techniques. In the study, we have found that the red colour of the glass is due to the presence of Cu^0 nanoparticles, the red glass layer has lower calcium content than the substrate glasses, which we found favours copper being present in the glass predominantly in Cu^+. They also contain tin and iron while lead, described in historical and modern documentation, was absent. Tin must have been added to the glass as a Sn^{2+} compound and acted as a reducing agent for copper. Iron is also a well-known reducing agent, but does not act as such in the red glasses studied here. However, it may have facilitated the reduction of copper to Cu^0 by promoting its incorporation into the glass as Cu^+ rather than Cu^{2+}.

* *Corresponding author.*
E-mail address: Trinitat.Pradell@upc.edu (T. Pradell).
https://doi.org/10.1016/j.bsecv.2023.07.005

El papel del estaño y el hierro en la producción de vidrio rojo de cobre en España en los siglos XIX y XX

Palabras clave:
Nanopartículas de cobre metálico
Cu, Fe K-edge y Sn L_3-edge
Micro-XAS
Micro-XRD
Vidrio de vidriera siglos XIX y XX
España

RESUMEN

Poco se sabe sobre los materiales utilizados en la fabricación de vidrios rojos planos en el siglo XIX y primera década del XX, por ello se han estudiado ocho fragmentos españoles de la época. Todos ellos están formados por una sola capa de vidrio rojo sobre un sustrato de vidrio incoloro. La composición química, el estado de oxidación, la naturaleza de los colorantes y los precipitados cristalinos se han determinado mediante una selección de técnicas microanalíticas. Hemos encontrado que la capa de vidrio rojo contiene nanopartículas de Cu^0, y que tiene un menor contenido de calcio menor que el vidrio sustrato, lo cual favorece que el cobre esté en el vidrio predominantemente como Cu^+. Tal y como está descrito en la documentación histórica y moderna contienen estaño y hierro, pero no se ha verificado la presencia de plomo. El estaño se agregó al vidrio como un compuesto Sn^{2+} y actuó como agente reductor del cobre. El hierro a pesar de ser un agente reductor, no actúa como tal en los vidrios rojos estudiados. Sin embargo, su presencia podría facilitar la reducción del cobre a Cu^0 al promover su incorporación al vidrio como Cu^+ en lugar de Cu^{2+}.

Introduction

Red copper glasses have been used in stained-glass windows in Europe since medieval times. The red colour is due to the presence of a low fraction (between 0.02% and 0.05% of the volume) of small metallic copper nanoparticles (below 50 nm in size) [1–6]; larger precipitates give a livery red colour, and the absorption and scattering of light by the particles dramatically reduces the transparency of the glasses [7,8].

Due to the low solubility of metals in a silicate melt, copper is mainly incorporated in its oxidized forms Cu^+ and Cu^{2+}. Subsequently, copper must be reduced to the metallic state, as nanoparticles, while avoiding the precipitation of other copper compounds such as cuprite (Cu_2O) or the development of large Cu^0 particles (livery red). Different strategies have been used throughout history, but mostly reducing agents were added to the melt [1,2,6,9]. To avoid the excess opacity due to the scattering of copper nanoparticles, the red glass was applied as only one or few layers on a substrate colourless glass and blown together.

Between the 13th and the 16th centuries, red glass was produced mainly in workshops in central Europe, and they exported the red glass throughout Europe. Recent analytical studies of red window glass from the 12th to the 17th century, including *striated* and *sandwich* types, revealed that *striated* glass was obtained by superimposing layers of oxidised copper-rich glass and reduced iron-rich glass; the interdiffusion of iron and copper across the glass boundary resulted in the oxidation of iron and reduction of copper and precipitation of metallic copper nanoparticles [6]. In contrast, sulphur appears to be the key element responsible for the development of the red colour of *sandwich* glass [10]. The oxidation of S^{2-} into S^{6+} induced the corresponding reduction of copper to the metallic state and precipitation of metallic copper nanoparticles.

The manufacture of red glass was kept secret until the 17th century, when the decline in coloured glass production and the fear of loss of knowledge led to a proliferation of various treatises. Neri wrote the first well-documented treatise on glass making, *L'art vetraria* (1612) [11] and later Kunckel's *Ars Vitraria Experimentalis* [12] and Pierre Le Vieil *L'Art de la Peinture sur verre et de la Vitrerie* [13], mainly based on Neri's work. The process of red glass production described involves mixing a *crystal* frit (soda rich mixed alkali glass) with copper and reducing agents. Two main recipes are described, one that incorporates tin and lead calx (an ash of molten lead and/or tin calcined at about 600 °C), burned iron or iron treated with vinegar, aqua fortis and aqua regia and calcined cream of tartar ($K_2CO_3{\cdot}1.5H_2O$) to burned copper, and a second type in which sulphur is also added. Recently, ignoring some inconsistencies in the chemical composition of the glass, red glass has been successfully replicated following Kunkel's recipes [14], firing the batch mixtures up to 1100 °C. A document written by Juan Danis in 1676, *Tratado de la fábrica del vidrio* [15], describes the need to reheat the glass after cooling in order to obtain the red colour.

Although the use of tin and lead calx is described already in these early treatises, their use has only been determined in the production of small volume objects between the 15th and the 18th centuries [16,17]. The colour of the glasses is red-brown and their composition is of soda-lime type, and contain iron (2–6% Fe_2O_3), lead (0.2–5.5% PbO) and tin (0.1–4.7% SnO_2) and also often antimony (0.2–1.1% Sb_2O_3). However, most of them were used to decorate glass objects rather than to colour the whole object, and none of them is flat glass for window use.

An 18th century treatise [18] describing the production of stain glass from the cathedral of Toledo, the addition of some tin-lead calx (3.8%PbO + SnO) to the red glass is mentioned. Nevertheless, the analysis of a red fragment from the cathedral of Toledo did not found either lead or tin.

Table 1 – Sample information. Dating of the buildings is indicated. However, after analysing the glass fragments TDM and SDC we have to date them in the 19th century (see text for more details).

Sample	Dating	Original location/collection	Window/artist
TDM	17th-c. building	Torroella de Montgri	Lower part of the window
SDC	14th-c. building reformed in the 18th c. Destroyed 1810 Closure 1835	Church of Sant Domenec. Cervera	Apse
Vic	1748–1753 Renewal 1883	Hospital Santa Creu. Vic	Dome
LGA	1876	Casa d'Empara. La Geltrú	Fragment
CB6	1880	Barcelona cathedral	Santa Tecla & Sant Jordi
SDPDM	1889	Seu de Palma de Mallorca	Trinity
CBCB	1905	Casa Bures. Barcelona	Skylight
CB7	1905	Museu del Disseny Barcelona. Cátedra Gaudí	Trichromacy fragment/Gaudí

Modern descriptions indicate the preferable use of a lead potash frit although a soda-lime frit with some boron was also used. Copper oxide, tin oxide and/or antimony oxide [9] or tin metal and, in some cases magnetite, were added [1] to the glass frit and fired to the melting temperature, then cooled and reheated between 500 °C and 650 °C to develop the red colour. Higher temperatures or longer firings may result in the loss of the red colour.

Little or nothing is known about the materials used in the manufacture of red window glass of the 18th, 19th and early 20th centuries. The glasses consist of a single thin surface layer of red glass on a colourless glass substrate, a type commonly known as *flashed* glass. In this work, the chemical composition, oxidation state and nature of colourants and the crystalline precipitates were determined in a series of eight Spanish historical samples, by combining a selection of microanalytical techniques: laser ablation inductively coupled plasma mass spectroscopy (LA-ICP-MS), field emission scanning electron microscopy (FE-SEM), microprobe, ultraviolet and visible spectroscopy (UV–Vis) and micro X-ray diffraction (micro-XRD) and micro X-ray absorption spectroscopy (micro-XAS) with synchrotron light.

Materials and experimental methods

Eight fragments of red glass were collected and analysed, details are shown in Table 1. The samples were selected from historic buildings, mainly from Catalonia, for which there is some documentation on the production and later restoration of the stained-glass windows.

Cross sections of the samples were obtained by embedding fragments in epoxy resin and polishing blocks down to 1 μm grade with a diamond paste. The polished sections were examined in reflected (Fig. 1) and transmitted light with an optical microscope (OM) Nikon Eclipse LV100D equipped with a camera Infinity 1.3C.

The cross sections were coated with a carbon layer (about 20 nm thick) and were examined in a crossbeam workstation (Zeiss Neon 40) equipped with scanning electron microscopy (SEM) GEMINI (Shottky FE) column with attached EDS (Ultim EDS Detector, Oxford Instruments), operated at 20 kV accelerating voltage with 1.1 nm lateral resolution, 20 nA current. Back Scattered Electron (BSE) images of the nanostructures were obtained at 20 kV acceleration voltage. A Focus Ion Beam (FIB, Ga ions, acceleration voltage 30 kV) was used to polish the surface and to obtain high resolution secondary electron images (5 kV) of the nanoparticles when they were too small to be observed directly on the mechanically polished cross section.

The chemical composition of the glasses was measured by LA-ICP-MS. The instrumentation used consists of a Resonetics M50E, ablation device, equipped with an excimer (ArF) laser working at 193 nm coupled with a Thermo Fisher Scientific ELEMENT XR mass spectrometer (details on the analytical methods are found in B. Gratuze [19]). The glasses were measured using an Electron Microprobe JEOL JXA-8230 from Scientific and Technological Centers from the University of Barcelona with five Wavelength-Dispersive X-ray Spectroscopy (WDS) spectrometers (probe current of 15 nA and calibration was performed using mineral and glass standards), to determine some elements not measured by LA-ICP-MS such as sulphur.

The nature of the particles present in the red glasses was determined by synchrotron-based micro-XRD. The micro-XRD patterns were obtained from thin cross sections (about 200 μm) cut from small fragments of the samples included in epoxy resin using a low speed diamond saw. Synchrotron micro-XRD patterns were collected in the Materials Science and Powder Diffraction beamline (MSPD BL04) [20], at the ALBA Synchrotron Light (Cerdanyola, Spain) in

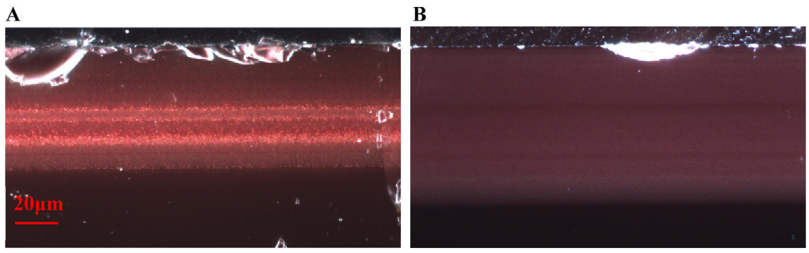

Fig. 1 – Dark field reflection optical microscope image of (A) TDM; (B) CB6 showing the presence of metallic copper nanoparticles.

transmission geometry, using 0.4246 Å wavelength (29.2 keV), a 20 μm × 20 μm spot size, and a CCD camera, SX165 (Rayonix, L.L.C., Evanston, IL) detector. The 2D images have been integrated using the d2Dplot program [21]. The XRD data has been identified using the Powder Diffraction File Database (PDF) from the International Centre for Diffraction Data (ICS) (ICCD, https://www.icdd.com).

Ultraviolet–Visible (UV–Vis) diffuse absorption measurements were obtained in transmission mode using a double beam spectrophotometer (Shimadzu 2700) recorded between 200 nm and 800 nm, and NIR transmittance measurements using a double beam spectrophotometer (Shimadzu 3600) recorded between 800 nm and 3000 nm.

Micro-XAS data of Fe, Cu at the K-edge and Sn at the L_3-edge were acquired at the ID21 beamline, ESRF [22]. X-rays were produced with an undulator, and their energy was adjusted using a Si (111) double crystal monochromator. For the analysis of glass samples, the beam was focused to 0.3 μm × 0.9 μm ($v \times h$) using a Kirkpatrick Baez mirror system. The samples were mounted vertically, at an angle of 62° with respect to the incident beam. X-rays was detected using a single energy-dispersive silicon drift detector (SGX, 80 mm^2) at 28° of the sample surface. XRF maps were first acquired at 9.5 keV, over 2D regions in order to locate elements (especially Cu, Fe and Sn) and identify regions of interest. The monochromator was calibrated using the first inflection point of the copper, iron and tin metal foils (maximum of the first derivative at 8979 eV for Cu foil, 7112 eV for Fe foil and 3929 eV for Sn foil) using Athena software [23]. Spectra of some reference powders (Cu_2S, CuO, Cu_2O, Fe_2O_3, Fe_3O_4, SnO and SnO_2) spread on a piece of tape and covered with an ultralene foil with an unfocussed beam (0.3 mm × 0.3 mm) in transmission mode were also acquired.

The copper speciation was obtained from the analyses of the Cu K-edge XAS spectra. Copper is either dissolved in the glass in the form Cu^+ and Cu^{2+}, or precipitated as Cu^0 nanoparticles EXAFS fitting was carried out with Artemis software. The spectrum is a linear combination of model compounds each weighted by each compound fraction with Artemis software [23]. Nevertheless, the lack of any longer-range order consistent with copper ions dissolved in the glass produces smooth EXAFS oscillations, making it difficult to fit more than the first shell. The first Cu—O and Cu—Cu shells were fitted taking as model compounds those of Cu_2O, CuO and metal Cu, each weighted by a compound fraction.

The pre-edge feature of the Fe K-edge absorption is particularly sensitive to the valence state and local geometry. The weighted peak position (centroid) is known to shift to higher energy as the ratio of ferric to ferrous iron increases [24] and the area gives an estimation of the coordination state. Based on the centroid, the oxidation state of iron in glasses can be calculated using the expression given in A. Fiege et al. [25]. The Fe K-edge XANES region has also been fitted using a Python code [26] developed following procedures described in literatures [24,27,28]. Considering that the data had standard resolution ($\Delta E = 0.5$ eV), the fitting incorporated some restrictions, the peaks are set Gaussian, the width fixed to 2.1 eV.

Tin speciation was obtained from the analysis of the Sn L-edge spectra to avoid the rather high energy required to collect the K-edge information (26,200 eV). Moreover, the Sn L_3-edge has been selected considering the low fluorescence yield of the L_1 and L_2-edges. A recent study [29] has shown that the L-edge is better than the K-edge for the determination of the oxidation state of tin in glasses. The absorption features of Sn L-edge absorption spectra of SnO, and SnO_2 have been assigned to corresponding electronic structures [30]. The $L_{3,2}$-edge white line corresponds to the transition from filled $2p_{3/2}$, $2p_{1/2}$ Sn states to empty $5d_{5/2}$, $5d_{3/2}$ Sn orbitals and the two fine structures appearing before the $L_{3,2}$ white lines were assigned to the $2p_{3/2} \rightarrow 5s_{1/2}$ transitions due to the s–p hybridization. The Sn L-edge spectra corresponding to Sn^{2+} and Sn^{4+} in glass are similar to those of crystalline SnO and SnO_2, but show smoother and broader absorption peaks [29].

Results

Table 2 shows the chemical composition of the glasses, red glass layer and colourless substrate glass. All the colourless substrate glasses are of the soda-lime type (10–15% Na_2O and CaO); they contain only about 0.5% SO_2, 0.1% Cl and 50 ppm P, indicating the use of synthetic soda (Na_2CO_3) in their production, which replaced plant ashes as a source of sodium. Synthetic soda was invented by the French chemist Nicholas Leblanc in 1791, an innovative process for making soda ash from salt and calcium carbonate, which was first used in the glass industry in 1835 [31,32]. This process was highly polluting (it produced hydrochloric acid) and was later replaced by the Solvay process patented in 1861 by Ernest and Alfred Solvay, which used salt, calcium carbonate, ammonia and charcoal [33]. In addition, the substrate glasses TDM, SDC and Vic contain relatively high amounts of arsenic (between 0.1 and 0.2% As_2O_3). The use of As_2O_3 as a refining agent was discovered a few years after the invention of Leblanc's salts [34]. Arsenic oxide was replaced by saltpetre (KNO_3) around 1870.

Table 2 – Major, minor and trace elements measured by LA-ICP-MS.

Sample	Colour	Na_2O	MgO	Al_2O_3	SiO_2	Cl	K_2O	CaO	Fe_2O_3	CuO	SnO_2	SO_3[a]	T_w
TDM	Red	17.1	0.25	1.27	73.1	0.10	0.46	4.55	0.50	1.03	1.16	–	1009
	Subs	16.2	0.20	0.98	72.8	0.23	0.93	7.42	0.09	0.00	0.01	–	1008
SDC	Red	13.0	0.06	0.86	75.9	0.20	0.13	5.03	2.22	0.46	1.95	–	1069
	Subs	11.9	0.14	0.68	70.3	0.06	0.51	16.0	0.30	0.01	0.04	0.64	1015
Vic	Red	13.3	0.11	0.78	74.2	0.10	0.09	7.94	1.06	0.94	1.34	–	1044
	Subs	11.0	0.15	0.56	73.5	0.07	0.09	14.2	0.20	0.01	0.01	0.43	1040
LGA	Red	12.9	0.04	0.78	76.8	0.19	0.22	5.55	1.31	1.07	1.00	–	1065
	Subs	11.5	0.11	1.01	73.9	0.05	0.28	12.7	0.25	0.04	0.03	0.44	1050
CB6	Red	12.4	0.05	0.64	78.3	0.19	0.20	5.08	1.31	0.75	0.93	–	1083
	Subs	11.6	0.13	1.46	73.4	0.06	0.47	12.4	0.28	0.05	0.05	0.55	1048
SDPDM	Red	12.6	0.04	0.64	77.1	0.21	0.12	5.44	1.11	1.38	1.26	–	1073
	Subs	12.4	0.22	1.56	71.5	0.14	0.51	13.0	0.29	0.06	0.05	0.52	1030
CBCB	Red	14.5	0.13	0.35	76.8	0.09	0.11	4.40	0.73	1.26	1.54	–	1030
	Subs	13.3	0.20	0.57	69.8	0.05	0.38	15.4	0.23	0.01	0.00	0.57	999
CB7	Red	15.5	0.24	0.41	74.7	0.16	0.16	5.65	0.70	0.84	1.51	–	1025
	Subs	12.7	0.45	0.55	71.0	0.04	0.24	14.7	0.25	0.01	0.01	0.47	1012

Sample	Colour	Li	B	P	Ti	Mn	Zn	As	Rb	Sr	Zr	Sn	Sb	Ba	Pb
TDM	Red	8	794	5	236	77	32	44	23	32	36	9140	14	68	705
	Subs	12	100	41	189	689	849	1596	8	84	30	82	899	1179	3706
SDC	Red	11	8	78	522	56	43	39	5	28	63	15358	7	83	101
	Subs	9	25	56	378	66	8	189	4	68	54	299	4	59	36
Vic	Red	12	24	128	452	43	48	36	5	39	27	10527	9	33	23
	Subs	10	23	53	196	39	7	788	4	164	18	118	2	29	26
LGA	Red	22	10	77	200	158	22	35	7	16	28	7838	6	40	60
	Subs	11	10	32	198	168	8	8	8	48	28	273	1	79	11
CB6	Red	14	12	94	239	395	25	41	8	21	39	7301	11	81	–
	Subs	10	6	50	179	82	9	15	12	61	28	372	1	104	8
SDPDM	Red	20	7	39	182	230	41	28	4	16	17	9941	6	54	29
	Base	14	7	52	188	989	9	8	12	98	29	398	7	459	61
CBCB	Red	8	15	–	181	82	18	26	4	22	19	12125	2	35	104
	Subs	11	23	52	206	32	10	2	6	136	21	21	0	40	31
CB7	Red	10	16	38	192	41	107	24	4	31	19	11870	2	30	34
	Subs	10	25	35	187	48	10	8	5	83	18	97	0	33	10

[a] Sulphur was measured by microprobe. T_w: the working temperature is the optimal temperature for blowing the glass has been calculated using the approximation given in [36].

Thermal decomposition of KNO_3 at 400 °C produces KNO_2 and O_2 (g) [35] which favours the release of bubbles. Consequently, SDC and Vic should be dated before 1870, LGA, CB6 and SDPDM after 1870. TDM contains many impurities, Mn, Zn, As, Sb, Ba, Pb, which seems to indicate a glass of low quality and probably an earlier date. Finally, CB7 and CBCB contain very few impurities, no more than a few dozen ppm of P, Cl, Mn, Zn, As, Sb, Ba, Pb. This is consistent with the dating of the glasses to the first decades of the 20th century. The working temperature (temperature required to blow the glass, T_w) of the 19th-century glasses is about 1050 °C, while for the 20th-century glasses it is slightly lower, about 1010 °C.

All the glasses show a single layer of red glass on the surface, i.e. *flashed* glasses. There are some important differences between the chemical composition of the red glass layers and the corresponding substrate colourless glasses. The red glasses contain copper and tin (≈0.5–1.4% CuO, 1–2% SnO_2), they also have a higher iron content (1–2% FeO in the 19th-century glasses and 0.7%FeO in the 20th-century glasses) and lower calcium content (5–7% CaO) than the corresponding substrate glasses (0.2% FeO and 12–15% CaO). Therefore, copper, tin and probably iron were added to obtain the red colour. The most important change is the addition of tin instead of sulphur (used before the 19th century) in the red glass, and also the addition of Fe (more in the 19th century than later in the 20th century red glasses). Both Sn^{2+} and Fe^{2+} are known reducing agents in glass, and may be involved in the reduction of copper to the metallic state.

In all the cases, the red colour of the glasses is due to the presence of small copper nanoparticles of typical sizes between 20 and 50 nm for all the red glass layers with the exception of TDM which has larger particles, between 50 and 150 nm, as shown in Fig. 2. No other crystalline precipitate was found.

UV–Vis is particularly useful for the identification of the presence of colouring cations in the glass, as well as the presence of cuprite and metallic copper nanoparticles. The UV–Vis absorption spectra corresponding to the glasses are shown in Fig. 3. Metallic copper nanoparticles show a Surface Plasmon Resonance (SPR) extinction band around 560 nm. The band is slightly red shifted (570 nm) for TDM, due to the larger particle sizes of the metallic copper nanoparticles.

In order to see the role of iron and tin in the formation of the metallic copper nanoparticles, the absorption spectra at

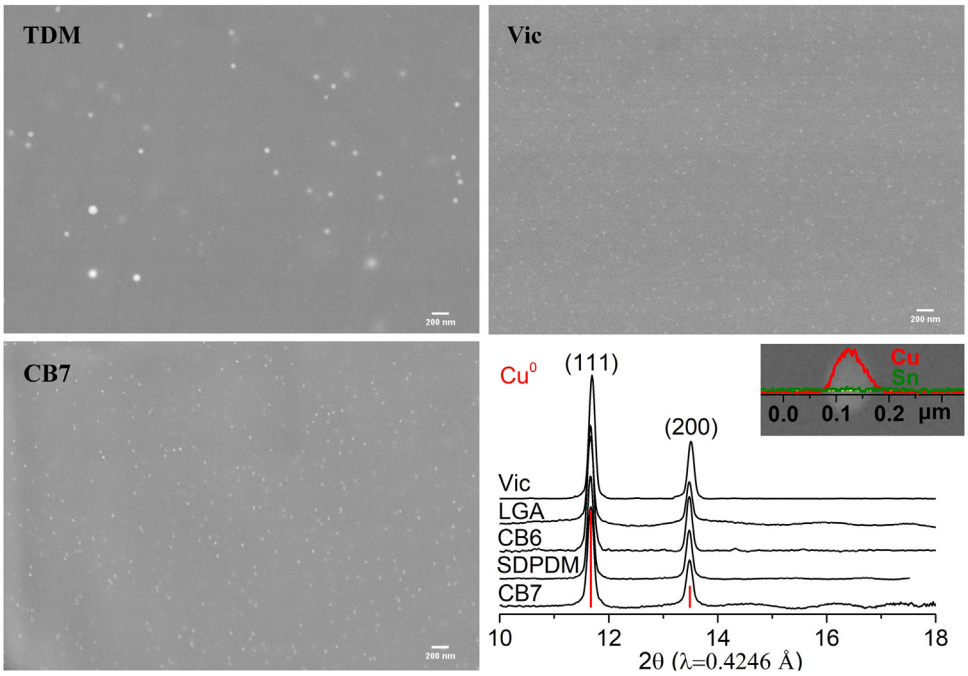

Fig. 2 – Secondary electrons FE-SEM images (TDM, Vic, CB7), micro-XRD patterns of the red glasses and line scan of a metallic copper nanoparticle of TDM.

Table 3 – Fitted Cu K-edge EXAFS data of SDC and CB7 red glass layers.

Sample	Shell	Model compound	Model parameters		Bond length	At. fraction	R_{factor}
			N	R (Å)	R (Å)	(%)	(%)
SDC	Cu—Cu	Cu^0	12	2.556	2.54(0)	100(16)	1.4
CB7	Cu—O	Cuprite	2	1.857	1.84(0)	49(6)	1.2
	Cu—Cu	Cu^0	12	2.556	2.53(0)	51(6)	

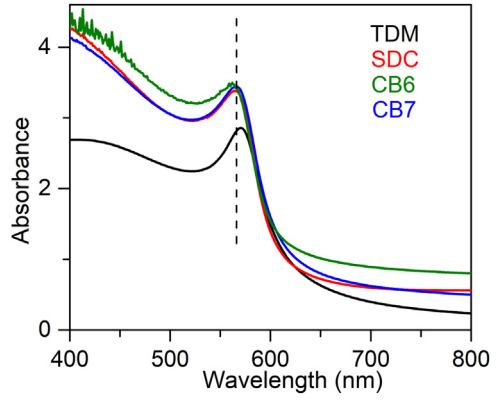

Fig. 3 – UV–Vis absorption spectra taken in transmission mode showing the SPR extinction band at 560 nm characteristic of metallic copper nanoparticles (20–50 nm). The spectrum corresponding to TDM appears slightly red shifted due to the large particle size (50–150 nm).

Table 4 – Fitted pre-edge peak center shift and Area of SDC and CB7 colourless substrate glasses and red glass layers, ε is the standard deviation of the fitted data.

	CE (eV) (ε = 0.15)	A (eV) (ε = 0.01)	$\%Fe^{3+}/\Sigma Fe$[a] (ε = 5%)
SDC			
Substrate	7113.2	0.20	52
Red	7112.3	0.14	8
CB7			
Substrate	7112.9	0.24	33
Red	7112.8	0.22	28

[a] Iron speciation calculated according to A. Fiege et al., 2017 [25].

the Fe and Cu K-edge and Sn L_3-edge were measured for some of the red and corresponding colourless substrate glasses, SDC from the 19th century and CB7 from the 20th century. The Cu K-edge XAFS taken from the red glasses and from the copper standards, Cu^0, Cu_2O and CuO are shown in Fig. 4A. In both spectra, the dominant contribution corresponds to metallic copper. Fig. 4B and Table 3 show the fit of the first shell data of the EXAFS region. Within the spectral resolution of XAS, SDC red glass is mostly metal while CB7 contains half of the copper as Cu^0 and the other half as Cu^+. Cu^{2+} is not found in the red glasses.

Fig. 5 and Table 4 show the Fe K-edge spectra and fitted data corresponding to the SDC and CB7 red glass layers and the substrate glasses. Iron is more reduced in the red glass

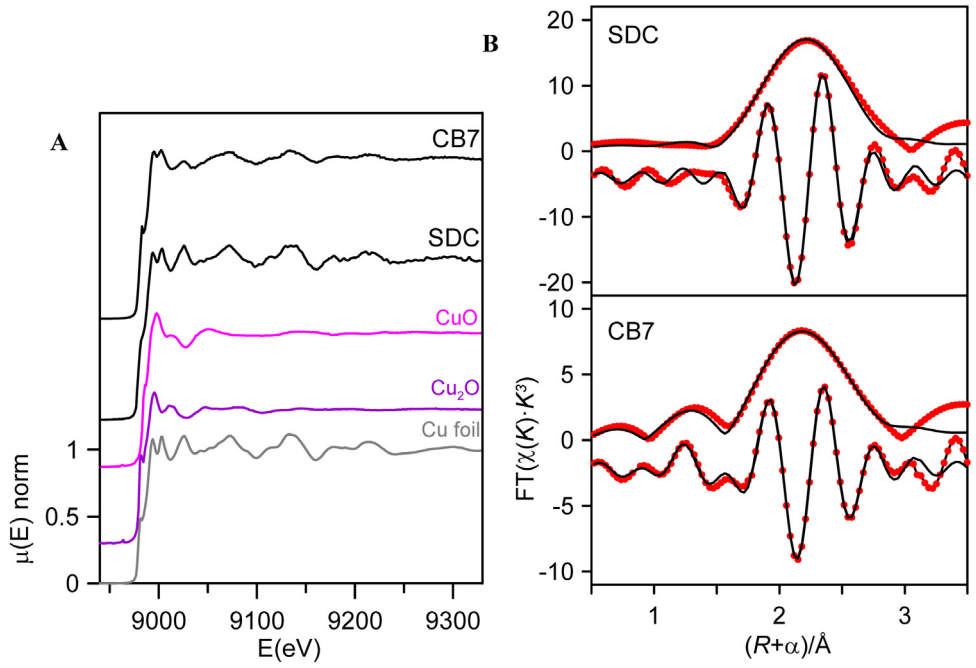

Fig. 4 – (A) Cu K-edge spectra of SDC, CB7 and Cu standards; (B) Cu K-edge EXAFS (dots) and curve fitting (line) for SDC and CB7 red glasses in R-space (FT magnitude and imaginary component). Data are k^3-weighted and not phase-corrected.

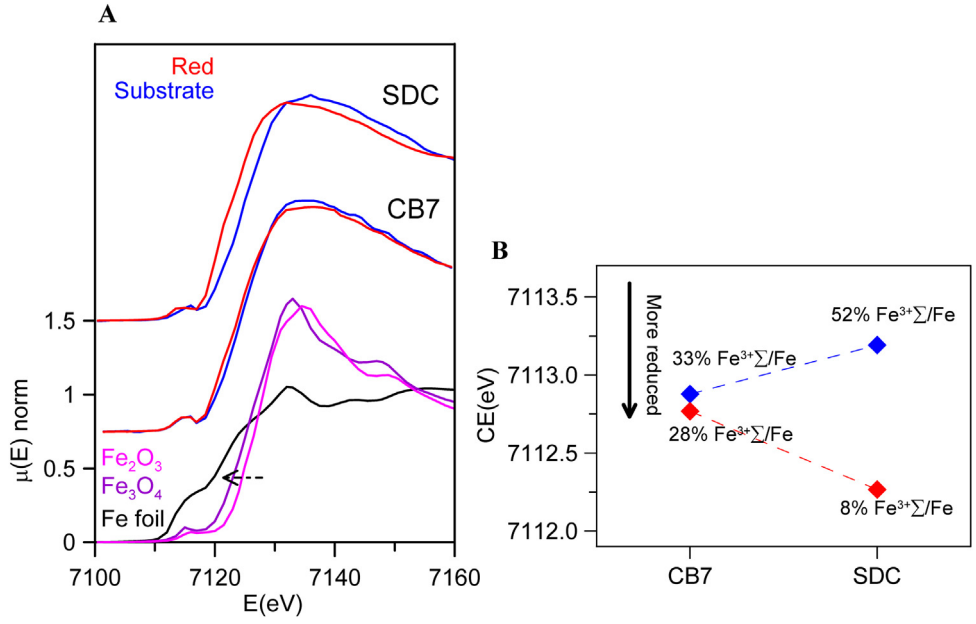

Fig. 5 – (A) Fe K-edge spectra of CB7 and SDC colourless substrate glasses and red glass layers (the red line and dots correspond to the red layer and the blue line and dots to the substrate transparent glass) and Fe standards. The edge shifts to higher energy as the iron becomes more oxidized; (B) pre-edge center shift (CE) of the glasses. The CE increases as the iron becomes more oxidized. The Fe^{3+} fraction has been calculated using the expression in A. Fiege et al. [25].

than in the substrate glass and in the red glass layers iron is also more oxidized in CB7 than in SDC.

Finally, Sn L_3-edge spectra from the substrate glass and red coloured layer were acquired from SDC and are shown in Fig. 6 together with the corresponding tin standards. The uncoloured substrate glasses contain only trace amounts of tin, 299 ppm for SDC, this is the reason why the corresponding data is very noisy. The Sn L_3-edge spectra corresponding to Sn^{2+} and Sn^{4+} in glass are similar to those of the crystalline oxides, SnO and SnO_2, but with smoother and broader absorption peaks [29]. We can clearly see that Sn^{4+} predominates in the red glass layer while Sn^{2+} predominates in the colourless substrate glass.

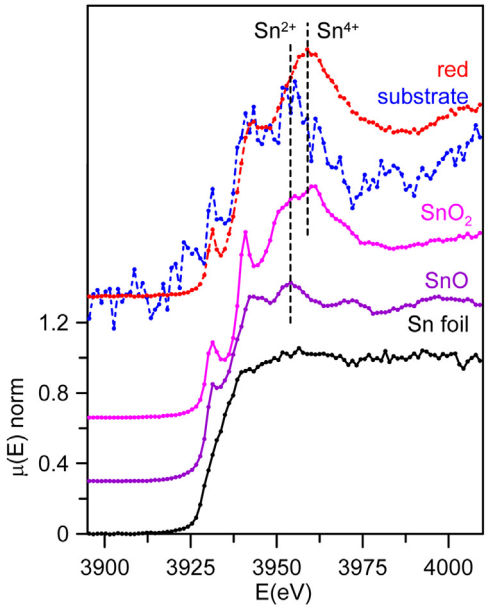

Fig. 6 – Sn L_3-edge spectra of SDC colourless substrate glass and red glass layer and Sn standards. Sn^{4+} predominates in the red glass layer while Sn^{2+} predominates in the colourless substrate glass.

Discussion

All the red flashed glasses from the 19th and 20th centuries are of the soda-lime type, and considering the low presence of ash components (P, S and Cl) manufactured from synthetic soda that was used in the glass industry since 1835 [31,32]. In addition, TDM, SDC and Vic glasses can be dated before 1870, while LGA, CB6 and SDPDM after 1870 (in good agreement with the official dating of the windows). Finally, CBCB and CB7 are dated to the very beginning of the 20th century, in 1905.

All the glasses have a single layer of red glass on the surface and are *flashed* glasses. The red glass layers contain copper and tin (≈0.5–1.4% CuO, 1–2% SnO_2), they also contain higher iron (1–2% FeO in the 19th-century glasses and 0.7% FeO in the 20th-century glasses) and lower calcium (5–7% CaO) than the corresponding substrate glasses (0.2% FeO and 12–15% CaO).

In a previous study, we demonstrated that copper and iron are more oxidised in Ca-rich glasses fired under the same conditions, oxidizing and then reducing [26]. The $Cu^+/(Cu^+ + Cu^{2+})$ was 70% in Ca-rich areas (about 23% CaO) and 90% in the Ca-poor areas (9% CaO) and the $Fe^{2+}/(Fe^{2+} + Fe^{3+})$ was 20% and 70%, respectively. In addition, a Mössbauer spectroscopy study of lime glasses [37] showed that the Fe^{3+} fraction increases with the CaO content of the glasses or the oxygen partial pressure of the firing. Therefore, decreasing the calcium content of red glasses favours both copper and iron to be present in a more reduced form.

The oxidation state of tin in soda-lime glasses has also been studied by Mössbauer spectroscopy [38]. A set of soda-lime glasses was produced by adding either a Sn^{4+} or a Sn^{2+} compound. Interestingly, when tin was added as Sn^{4+}, tin was present as Sn^{4+} in the glass whereas if it was added as Sn^{2+}, only half of the tin was still present as Sn^{2+} in the glass, the other half was already as Sn^{4+}. No differences in the behaviour were found for tin contents ranging from 0.4 to 6% SnO_2 or SnO.

Table 5 – Chemical composition of the red glasses.

	at% Sn	at% Fe	at% Cu	Sn/Cu
TDM	0.22	0.10	0.24	0.9
SDC	0.33	0.49	0.12	2.8
Vic	0.22	0.28	0.25	0.9
LGA1	0.17	0.31	0.28	0.6
CB6	0.14	0.30	0.17	0.8
SPDM	0.20	0.24	0.33	0.6
CBCB	0.19	0.19	0.29	0.7
CB7	0.25	0.17	0.24	1.0

Due to the extremely low solubility of metals in silicate glass, copper must be incorporated into the glass in its ionic form, Cu^+ and/or Cu^{2+}, which requires an oxidizing atmosphere during the firing. The process of red glass production described in the historical and modern documents involves mixing the glass with copper and reducing agents such as tin, lead, iron and/or calcined cream of tartar ($K_2CO_3{\cdot}1.5H_2O$) and firing at high temperatures [1,11,12,14]. According to historical treatises, the ingredients were pretreated (burned copper, vinegar, aqua fortis, or aqua regia treated iron, tin-lead ashes), while more recent descriptions indicated the addition of tin oxide, magnetite and in some cases directly as metal (Sn^0) [1,9]. Our glasses do not contain lead, and only tin and iron were added as reducing agents.

Our data have shown that in the red glass, copper appears as Cu^+ and Cu^0 while tin is present mainly in its oxidized form Sn^{4+}. Consequently, tin acted as a reducing agent, which requires tin to be incorporated into the glass as Sn^{2+}. The addition of other reducing agents, such as $K_2CO_3{\cdot}1.5H_2O$ to the glass melt, as described in historical and modern documents, would favour the incorporation of tin as Sn^{2+} into the glass. It has been found [38] that when tin is added in the form of SnO, only half of the tin remains in the glass as Sn^{2+}, so that a tin to copper ratio of 2:1 is required to reduce all the copper. Therefore, the relative amount of the different ions involved must be taken into account. Table 5 shows the atomic concentration of tin, iron and copper in the red glasses. In CB7 with a Sn:Cu = 1:1, only half of the copper is reduced to the metallic state, while in SDC with Sn:Cu = 2:1, all copper is reduced to the metallic state. To obtain a red glass, it is therefore necessary to use a Sn^{2+} compound or metallic tin, or to add some reducing agents such as $K_2CO_3{\cdot}1.5H_2O$ to the melt, as described in the documentation. Once tin is oxidised to Sn^{4+}, it is quite soluble in alkaline glasses [5] and remains dissolved in the red glass. The predominance of Sn^{2+} in the substrate glass indicates reducing conditions during production, which is probably also aided by the low tin content (200–300 ppm).

Iron in SDC is mainly present in its reduced form (about 90% Fe^{2+}) and cannot have acted as a reducing agent for copper. Consequently, the role of iron is less clear. However, since iron in a calcium poor soda-lime glass tends to be present in its more reduced state Fe^{2+}, copper may be more likely present in the glass as Cu^+ rather than Cu^{2+}, as we have seen occurring [26]. Iron may then have an indirect role in the production of

red glass by preventing the presence of copper as Cu^{2+}, thus facilitating the reduction of copper to the metallic state. In addition, we have observed that the iron content of red glasses decreases slightly in the 20th century.

The 19th century marks an important change in the production technology of copper red glasses. This coincides with scientific advances in glass production such as the use of synthetic soda, the use of As_2O_3 and later of KNO_3 as refining agents.

Conclusions

Little or nothing is known about the materials used in the manufacture of red window glass in the 18th and 19th centuries and the first decade of the 20th century. A selection of seven copper red glasses was studied, all of them consisting of a single thin surface layer of red glass on a colourless glass substrate, a type commonly known as *flashed* glass. The chemical composition of the substrate colourless glasses indicated that they were all obtained from synthetic soda which was not used before 1835; the presence/absence of arsenic added to the glass as a fining agent, allowed dating three of them before 1870 and three after 1870, the other two were produced in 1905. The red colour of the glass is due to the presence of metallic copper nanoparticles (size 20–50 nm). Contrary to the red copper glasses produced between the 13th and 17th centuries, the composition of red glass layers is different from those of the substrate glasses. The red glass shows low-calcium content (about 5% CaO) which causes both copper and iron to be present in the glass predominantly in their reduced form, Cu^{+} and Fe^{2+}. Red glasses contained copper, tin and iron while lead, described in historical and modern documentation was absent.

Our data has shown that tin is present mainly in its oxidized form Sn^{4+}, in the red glass, while copper is present as Cu^{+} and metallic copper; the more the copper is reduced, the more the iron in the glass is reduced. Consequently, tin acted as a reducing agent, which requires tin to be incorporated into the glass as Sn^{2+}. The addition of other reducing agents such as $K_2CO_3{\cdot}1.5H_2O$, as described in historical and modern documents, would promote the incorporation of tin as Sn^{2+} into the glass. The role of iron is less clear, but since iron is also preferentially incorporated in a low-calcium glass as Fe^{2+}, it may prevent the incorporation of copper as Cu^{2+}, facilitating the reduction of copper to the metallic state.

Funding

This work received financial support from MINECO (Spain) (grant PID2019-105823RB-I00), the Generalitat de Catalunya (grant 2021 SGR 00343) and structural analysis of historical materials, 2025 https://doi.org/10.15151/ESRF-ES-879445008.

Conflict of interest

We have no conflict of interest.

Acknowledgements

The XAS experiments were performed at ID21 Beamline at ESRF with the collaboration of ESRF Staff, through the proposal HG-172. Micro-XRD experiments were performed at BL04 (MSPD) Beamline at ALBA synchrotron facility with the collaboration of Alba Staff.

REFERENCES

[1] W.A. Weyl, Coloured Glasses, Reprint by Society of Glass Technology, Sheffield, 1951, pp. 2016.
[2] S. Ishida, M. Hayashi, N. Takeuchi, M. Wakamatsu, Role of Sn^{2+} in development of red colour during reheating of copper glass, J. Non-Cryst. Solids 95–96 (1987) 793–800, http://dx.doi.org/10.1016/S0022-3093(87)80683-X.
[3] I.C. Freestone, Composition and microstructure of early opaque red glass in Early Vitreous Materials, in: M. Bimson, I.C. Freestone (Eds.), British Museum Occasional Paper 56, London, 1987, pp. 173–191, ISBN 13 9780861590568.
[4] I. Nakai, C. Numako, H. Hosono, K. Yamasaki, Origin of the red color of satsuma copper-ruby glass as determined by EXAFS and optical absorption spectroscopy, J. Am. Ceram. Soc. 82 (3) (1999) 689–695, http://dx.doi.org/10.1111/j.1151-2916.1999.tb01818.x.
[5] F. Farges, M.P. Etcheverry, A. Scheidegger, D. Grolimund, Speciation and weathering of copper in "copper red ruby" medieval flashed glasses from the Tours cathedral (XIII century), Appl. Geochem. 21 (10) (2006) 1715–1731, http://dx.doi.org/10.1016/j.apgeochem.2006.07.008.
[6] J.J. Kunicki-Goldfinger, I.C. Freestone, I. McDonald, J.A. Hobot, H. Gilderdale-Scott, T. Ayers, Technology, production and chronology of red window glass in the medieval period-rediscovery of a lost technology, J. Archaeol. Sci. 41 (2014) 89–105, http://dx.doi.org/10.1016/j.jas.2013.07.029.
[7] T. Pradell, Lustre and nanostructures-ancient technologies revisited, in: P. Dillmann, L. Bellot-Gurlet, I. Nenner (Eds.), Nanoscience and Cultural Heritage, Atlantis Press, Paris, 2016, http://dx.doi.org/10.2991/978-94-6239-198-7_1.
[8] G. Li, Y. Lei, The computational simulation of the reflection spectra of copper red glaze, AIP Adv. 12 (9) (2022) 095319, http://dx.doi.org/10.1063/5.0095570.
[9] T. Bring, B. Jonson, L. Kloo, J. Rosdahl, R. Wallenberg, Colour development in copper ruby alkali silicate glasses. Part 1. The impact of tin(II) oxide, time and temperature, Glass. Technol. Eur. J. Glass Sci. Technol. A 48 (2) (2007) 101–108.
[10] M.Y. Yuan, J. Bonet, M. Cotte, N. Schibille, B. Gratuze, T. Pradell, The role of sulphur in the early production of copper red stained glass, Ceram. Int. (2023), http://dx.doi.org/10.1016/j.ceramint.2023.02.236.
[11] M. Cable, in: M. Cable (Ed.), The World's Most Famous Book on Glassmaking: The Art of Glass by Antonio Neri, Christopher Merrett (Transl.), The Society of Glass Technology, Sheffield, 2001, ISBN: 090068237X.
[12] J. Kunckel, Ars Vitraria Experimentalis, Oder Vollkommene Glasmacher-Kunst (Franckfurt und Leipzig, 1679) Deutches Textarchiv. http://www.deutschestextarchiv.de/kunckel_glasmacher_1679.
[13] P. Le Vieil, L'Art de la Peinture sur verre et de la Vitrerie, France, 1774. ISBN 10: 2019937972.
[14] M. Vilarigues, A. Ruivo, T. Hagendijk, M. Bandiera, M. Coutinho, L.C. Alves, S. Dupré, Red glass in Kunckel's Ars Vitraria Experimentalis: the importance of temperature, Int. J. Appl. Glass Sci. (2022) 1–15, http://dx.doi.org/10.1111/ijag.16605.

[15] V. Nieto, El tratado de la fabrica del vidrio de Juan Danis y el Modo de hacer vidrieras de Francisco Herranz, Archivo español de Arte 40 (159) (1967) 273–303.
[16] M. Bandiera, M. Verità, S. Zecchin, M. Vilarigues, Some secrets of Renaissance Venetian opaque red glass revealed by analyses and glassmaking treatises, Glass Technol. Eur. J. Glass Sci. Technol. A 62 (1) (2021) 24–33, http://dx.doi.org/10.13036/1753354662.1.001.
[17] L. Dussubieux, B. Gratuze, Chemical composition of 16–18th-century glass beads excavated in Paris, BEADS: J. Soc. Bead Res. 24 (2012) 6, https://surface.syr.edu/cgi/viewcontent.cgi?article=1212&context=beads.
[18] A. La Iglesia, M.C. López de Azcona, F.M. Martín, El "Tratado secreto de pintar a fuego las vidrieras de colores" de F Sánchez Martínez, 1718. Composición Química de algunos vidrios antiguos de la Catedral de Toledo, Bol. Soc. Esp. Cerám. Vidrio 33 (6) (1994) 327–331, http://boletines.secv.es/upload/199433327.pdf.
[19] B. Gratuze, Glass characterization using laser ablation-inductively coupled plasma-mass spectrometry methods, in: L. Dussubieux, M. Golitko, B. Gratuze (Eds.), Recent Advances in Laser Ablation ICP-MS in Archaeology, Springer Verlag, Natural Sciences in Archaeology, Berlin Heidelberg, 2016, pp. 179–196, http://dx.doi.org/10.1007/978-3-662-49894-1 (Chapter 12).
[20] F. Fauth, I. Peral, C. Popescu, M. Knapp, The new material science powder diffraction beamline at ALBA synchrotron, Powder Diffr. 28 (S2) (2013) S360–S370, http://dx.doi.org/10.1017/S0885715613000900.
[21] O. Vallcorba, J. Rius, d2Dplot: 2D X-ray diffraction data processing and analysis for through the substrate microdiffraction, J. Appl. Cryst. 52 (2019) 478–484, http://dx.doi.org/10.1107/S160057671900219X.
[22] M. Cotte, E. Pouyet, M. Salomé, C. Rivard, W. De Nolf, H. Castillo-Michel, T. Fabris, et al., The ID21 X-ray and infrared microscopy beamline at the ESRF: status and recent applications to artistic materials, J. Anal. At. Spectrom. 32 (2017) 477–493, http://dx.doi.org/10.1039/C6JA00356G.
[23] B. Ravel, M. Newville, ATHENA, ARTEMIS, HEPHAESTUS: data analysis for X-ray absorption spectroscopy using IFEFFIT, J. Synchrotron Radiat. 12 (2005) 537–541, http://dx.doi.org/10.1107/S0909049505012719.
[24] M. Wilke, F. Farges, P.E. Petit, G.E. Brown, F. Martin, Oxidation state and coordination of Fe in minerals: an Fe K-XANES spectroscopic study, Am. Miner. 86 (5) (2001) 714–730, http://dx.doi.org/10.2138/am-2001-5-612.
[25] A. Fiege, P. Ruprecht, A.C. Simon, A.S. Bell, J. Göttlicher, M. Newville, T. Lanzirotti, G. Moore, Calibration of Fe XANES for high precision determination of Fe oxidation state in glasses: comparison of new and existing results obtained at different synchrotron radiation sources, Am. Miner. 102 (2017) 369–380, http://dx.doi.org/10.2138/am-2017-E102410.
[26] M.Y. Yuan, J.Y. Hou, G. Gorni, D. Crespo, Y. Li, T. Pradell, Jun ware glaze colours: an X-ray absorption spectroscopy study, J. Eur. Ceram. Soc. 42 (6) (2022) 3015–3022, http://dx.doi.org/10.1016/j.jeurceramsoc.2022.02.016.
[27] M. Wilke, G.M. Partzsch, R. Bernhardt, D. Lattard, Determination of the iron oxidation state in basaltic glasses using XANES at the K-edge, Chem. Geol. 220 (2005) 143–161, http://dx.doi.org/10.1016/j.chemgeo.2005.03.004.
[28] A. Boubnov, H. Lichtenberg, S. Mangold, J.D. Grunwaldt, Identification of the iron oxidation state and coordination geometry in iron oxide- and zeolite-based catalysts using pre-edge XAS analysis, J. Synchrotron Radiat. 22 (2015) 410–426, http://dx.doi.org/10.1107/S1600577514025880.
[29] H. Masai, T. Ina, S. Okumura, K. Mibu, Validity of valence estimation of dopants in glasses using XANES analysis, Sci. Rep. 8 (2018) 415, http://dx.doi.org/10.1038/s41598-017-18847-0.
[30] Z.L. Liu, K. Handa, K. Kaibuchi, Y. Tanaka, J. Kawai, Comparison of the Sn L edge X-ray absorption spectra and the corresponding electronic structure in Sn, SnO, and SnO_2, J. Electron Spectrosc. Relat. Phenom. 135 (2004) 155–158, http://dx.doi.org/10.1016/j.elspec.2004.03.002.
[31] F. Aftalion, A History of the International Chemical Industry (Chemical Science in Society) O.T. Bentey (Transl.), University of Pennsylvania Press, Philadelphia, 1991, pp. 11–13, ISBN 13: 978-0-8122-1297-6.
[32] D. Dungworth, The value of historic window glass, Hist. Environ. 2 (1) (2011) 21–48, http://dx.doi.org/10.1179/175675011X12943261434567.
[33] D.S. Kostick, The origin of the U.S. natural and synthetic soda ash industries, in: Proceedings First International Soda Ash Conference, vol. I, Laramie, Wyoming, 1998, pp. 11–35.
[34] S. Muspratt, Chemistry, Theoretical Practical and Analytical, as Applied and Relating to the Arts and Manufactures, Vol. 2, William Mackenzie, Glasgow, Scotland, 1860, https://digital.sciencehistory.org/works/ysz6nva.
[35] C.M. Kramer, Z.A. Munir, Thermal decomposition of $NaNO_3$ and KNO_3, in: ECS Proceedings Volumes, vol. 9, 1981, pp. 494–505, http://dx.doi.org/10.1149/198109.0494PV.
[36] A. Fluegel, Glass viscosity calculation based on a global statistical modelling approach, Glass Technol.: Eur. J. Glass Sci. Technol. A 48 (1) (2007) 13–30, https://glassproperties.com/viscosity/.
[37] N. Iwamoto, Y. Tsunawaki, H. Nakagawa, T. Yoshimura, N. Wakabayashi, Investigation of calcium-iron-silicate glasses by the Mössbauer method, J. Non-Cryst. Solids 29 (3) (1978) 347–356, http://dx.doi.org/10.1016/0022-3093(78)90155-2.
[38] M.H. Krohn, J.R. Hellmann, B. Mahieu, C.G. Pantano, Effect of tin-oxide on the physical properties of soda-lime–silica glass, J. Non-Cryst. Solids 351 (6–7) (2005) 455–465, http://dx.doi.org/10.1016/j.jnoncrysol.2005.01.050.